Research

New Phytologist

Tomato SlGSTU38 interacts with the PepMV coat protein and promotes viral infection

Eduardo Méndez-López[1], Livia Donaire[1], Blanca Gosálvez[1], Pedro Díaz-Vivancos[2], M. Amelia Sánchez-Pina[1], Jens Tilsner[3,4] and Miguel A. Aranda[1]

[1]Department of Stress Biology and Plant Pathology, CEBAS-CSIC, Campus Universitario de Espinardo, 30100 Murcia, Spain; [2]Department of Plant Breeding, CEBAS-CSIC, Campus Universitario de Espinardo, 30100 Murcia, Spain; [3]Biomedical Sciences Research Complex, The University of St. Andrews, St. Andrews, KY16 9ST, UK; [4]Cell and Molecular Sciences, The James Hutton Institute, Dundee, DD2 5DA, UK

Author for correspondence:
Eduardo Méndez-López
Email: fmendez@cebas.csic.es

Received: *11 August 2022*
Accepted: *19 December 2022*

New Phytologist (2023) **238:** 332–348
doi: 10.1111/nph.18728

Key words: host factor, PepMV, potexvirus, redox homeostasis, resistance, stress response, viral replication complex (VRC).

Summary

- Pepino mosaic virus (PepMV) is pandemic in tomato crops, causing important economic losses world-wide. No PepMV-resistant varieties have been developed yet. Identification of host factors interacting with PepMV proteins is a promising source of genetic targets to develop PepMV-resistant varieties.
- The interaction between the PepMV coat protein (CP) and the tomato glutathione *S*-transferase (GST) SlGSTU38 was identified in a yeast two-hybrid (Y2H) screening and validated by directed Y2H and co-immunoprecipitation assays. *SlGSTU38*-knocked-out Micro-Tom plants (*gstu38*) generated by the CRISPR/Cas9 technology together with live-cell imaging were used to understand the role of SlGSTU38 during infection. The transcriptomes of healthy and PepMV-infected wild-type (WT) and *gstu38* plants were profiled by RNA-seq analysis.
- SlGSTU38 functions as a PepMV-specific susceptibility factor in a cell-autonomous manner and relocalizes to the virus replication complexes during infection. Besides, knocking out *SlGSTU38* triggers reactive oxygen species accumulation in leaves and the deregulation of stress-responsive genes.
- SlGSTU38 may play a dual role: On the one hand, SlGSTU38 may exert a proviral function depending on its specific interaction with the PepMV CP; and on the other hand, SlGSTU38 may delay PepMV-infection sensing by participating in the redox intracellular homeostasis in a nonspecific manner.

Introduction

Pepino mosaic virus (PepMV; genus *Potexvirus*, family *Alphaflexiviridae*) was described for the first time in 1999 as a tomato pathogen in the Netherlands (van der Vlugt *et al.*, 2000, 2002), since then spreading rapidly to the main tomato-producing areas world-wide (Hanssen & Thomma, 2010; Gómez *et al.*, 2012). PepMV-induced symptoms may vary depending on the virus isolate and environmental conditions (Hanssen & Thomma, 2010; Sempere *et al.*, 2016), but very frequently include irregular pigment distribution during fruit ripening, which severely affects fruit quality and marketability. PepMV is transmitted mechanically in a very efficient manner, and its control is difficult, mainly relying on prophylaxis. Cross-protection against PepMV has been described (Hanssen *et al.*, 2010; Agüero *et al.*, 2018), and it is being widely adopted in Europe, as no commercial resistant tomato varieties have been deployed yet. This is despite the repeated attempts to identify sources of resistance to PepMV in the natural diversity of *Solanum* spp. (e.g. Soler-Aleixandre *et al.*, 2007). The identification of new sources of resistance could significantly contribute to the improvement of PepMV control.

The PepMV genome is a positive-sense single-stranded RNA molecule with a 5′cap, a polyA tail, and five ORFs encoding the RNA-dependent RNA polymerase (RdRp), the triple gene block (TGB) proteins 1, 2, and 3, and the coat protein (CP). The CP oligomerizes to form the capsid that protects the viral RNA in the viral particle (Agirrezabala *et al.*, 2015). The PepMV CP has three major regions, an N-terminal flexible arm responsible for lateral CP–CP contacts in the virion, a core region with an RNA-binding pocket, and a C-terminal extension that protrudes from the core region, participating in longitudinal CP–CP contacts. The overall topology of the PepMV CP is conserved in all the CPs of flexuous filamentous plant viruses and some nucleocapsid proteins of animal viruses (Agirrezabala *et al.*, 2015; Zamora *et al.*, 2017). The PepMV CP is also an RNA silencing suppressor that interacts with TGB1 (Mathioudakis *et al.*, 2014). Potexvirus TGB proteins are critical for viral RNA intra and intercellular trafficking (Park *et al.*, 2014) and are involved in reorganizing the cell cytoskeleton and recruiting endoplasmic reticulum (ER) and Golgi apparatus (GA) vesicles into the viral replication complexes (VRCs; Tilsner *et al.*, 2012, 2013; Ruiz-Ramón *et al.*, 2019). For the model potexvirus potato virus

X (PVX), TGB2 and 3 remodel the ER at plasmodesmata (PD) entrances to form membrane structures where viral replication takes place, possibly facilitating co-replicational cell-to-cell transport; TGB1 and CP have a critical role in directing the viral RNA through the PD (Tilsner *et al.*, 2013). In parallel, cytoplasmic TGB2/3 vesicles aggregate onto TGB1-reorganized actin filaments to build the VRC, which shows regionalization of its components (Tilsner *et al.*, 2012). PepMV induces similar bodies in infected cells that are likely to be VRCs (Minicka *et al.*, 2015; Ruiz-Ramón *et al.*, 2019). Viral replication complexes (VRCs) are cellular pseudo-organelles whose formation and activity implies deep ultrastructural changes (Nguyen-Dinh & Herker, 2021; Sánchez-Pina *et al.*, 2021) and likely the recruitment of a multitude of host factors. However, the number of host factors known to play a role in the potexvirus biology is still very limited, including few host proteins that interact with the CP (Candresse *et al.*, 2010; Cho *et al.*, 2012; Mathioudakis *et al.*, 2012; Park & Kim, 2013; Lim *et al.*, 2014; Choi *et al.*, 2016).

Glutathione *S*-transferases (GSTs) are universal in eukaryotes and prokaryotes and are encoded by a very large gene family organized into 36 classes, with 14 of them present in eukaryote photosynthetic organisms including the tau (GSTU) class (Vaish *et al.*, 2020). Plant GSTs have different functions. GSTs catalyze the conjugation of the tripeptide glutathione (γ-L-glutamyl-L-cysteinyl-glycine; GSH) to detoxify electrophilic toxic molecules such as xenobiotics, promoting their vacuolar sequestration (Martinoia *et al.*, 1993). Some GSTs have glutathione peroxidase activity (Bartling *et al.*, 1993; Wagner *et al.*, 2002; Dixon *et al.*, 2009) and participate in antioxidative defense. GSTs are also involved in secondary metabolism, growth and development, and response against biotic and abiotic stresses (Vaish *et al.*, 2020). A relationship between redox balance, GST activity level, and resistance to pathogens has been observed in different crop cultivars (Gullner *et al.*, 2018). GSTs may also modulate protein *S*-glutathionylation, a post-translational modification that may have a protective effect under oxidative conditions, or may regulate the activity of the modified protein (Grek *et al.*, 2013). In particular, a *Nicotiana benthamiana* D. GST, NbGSTU4, has been described to bind to the bamboo mosaic virus (BaMV) genomic 3′ UTR, and *NbGSTU4* gene silencing results in a decrease in BaMV replication (Chen *et al.*, 2013). Other antioxidant proteins have been identified to interact with PepMV proteins. Tomato catalase 1 (CAT1) interacts with PepMV TGB1, and silencing of the CAT1 coding gene negatively affects viral accumulation; moreover, an increase in catalase activity was observed in PepMV-infected plants and plants expressing TGB1 (Mathioudakis *et al.*, 2013). The same research group also described the interaction between PepMV TGB1 and a thioredoxin, but the biological function of this interaction remains unknown (Mathioudakis *et al.*, 2018).

In this work, we identified and validated the interaction between PepMV CP and a tomato GST belonging to the *tau* class (SlGSTU38), showing that this interaction is specific among the tomato GSTUs that are phylogenetically close to SlGSTU38. We also show here that SlGSTU38 localizes within the PepMV VRCs. We generated SlGSTU38-knocked-out tomato (cv Micro-Tom) plants using the CRISPR/Cas9 technology; these plants showed loss of susceptibility to PepMV, indicating that SlGSTU38 is a susceptibility factor for PepMV. We also compared the transcriptomic profiles of healthy and PepMV-infected *gstu38* and wild-type (WT) plants, and we observed a preactivation of immune and stress responses in healthy *gstu38* plants. Tomato plants edited in *SlGSTU38* may be a valuable source of resistance to PepMV.

Materials and Methods

Plant and virus material

Solanum lycopersicum L. (cv Money Maker and cv Micro-Tom) and *Nicotiana benthamiana* D. plants were used in this work. All the plants grew in a growth chamber or in a controlled environment glasshouse set at 25°C with a 16 h : 8 h, light : dark cycle. The virus isolate used was PepMV-Sp13 (Aguilar *et al.*, 2002), and the agroinfective clone pBPepXL6 derived from it (Sempere *et al.*, 2011) as initiator of PepMV infections. Tobacco mosaic virus (TMV; PV-1252) and PVX (PV-0017) isolates were acquired from the DSMZ collection.

Tomato cDNA library and yeast two-hybrid screening

The tomato cDNA normalized library was built by Evrogen (Moscow, Russia), and the Y2H screening was conducted by Dualsystems Biotech (Zürich, Switzerland) following its own protocol (Supporting Information Methods S1).

DNA constructs

The Gateway cloning technology (Invitrogen) was used to prepare most of the DNA constructs. The primers and templates used for the amplification of the coding sequences (CDSs) of PepMV *CP* and *SlGSTUs* genes are shown in Tables S1 and S2. The Gateway amplicons were cloned into the donor vector pDONR/Zeo after the BP reaction (Invitrogen). DNA preparations of the entry vectors were used for LR reactions (Invitrogen), for cloning into the destination vectors pGADT7 and pGBKT7-GW (Lu *et al.*, 2010) for Y2H; pGWB2, pGWB452 and pGWB455 (Nakagawa *et al.*, 2007a,b) for CoIP, and protein localization. The resulting expression vectors are shown in Table S2. All of these expression vectors were used to transform C58C1 *Agrobacterium tumefaciens* cells, except pGADT7 and pGBKT7-based vectors for Y2H, which were used to transform AH109 yeast cells (Gietz & Schiestl, 1994).

For the generation of the CRISPR/Cas9 plasmid pA60-GST19, we designed a guide RNA (gRNA) by submitting the *SlGSTU38* CDS to the online tool Breaking Cas (Oliveros *et al.*, 2016). After selecting the gRNAs with no off-targets, secondary structures of the candidate gRNAs fused to the RNA scaffold were predicted using the MFOLD web server (http://www.unafold.org/) (Zuker, 2003); we chose the guide with optimal folding (Liang *et al.*, 2016) and located as upstream of the

SlGSTU38 CDS as possible; we named it GST19. Two complementary primers (CE1981 and CE1982; Table S1) overlapping the GST19 sequence with a 5′ cohesive *Bbs*I terminus were annealed and cloned into the *Bbs*I-treated pBS_KS_gRNA_BbsI plasmid (Abiopep SL, Murcia, Spain) (Pechar *et al.*, 2022) resulting in the plasmid named pA58-GST19, whereby the GST19 gRNA was fused to the RNA scaffold that binds the Cas9 nuclease. The plasmid pA58-GST19 and pK7_CAS9-TPC_MCS (Abiopep SL) (Pechar *et al.*, 2022), a binary expression vector carrying the Cas9 nuclease gene and the *neomycin phosphotransferase II* (*nptII*) plant transfection reporter gene conferring kanamycin resistance, were digested with *Spe*I and *Kpn*I. After electrophoretic fractionation and gel purification of the fragments of interest, the GST19 gRNA fused to the RNA scaffold was cloned into the plasmid pK7_CAS9-TPC_MCS resulting in the binary expression vector pA60-GST19. Then, GV3101 *A. tumefaciens* cells were transformed with pA60-GST19.

Directed yeast two-hybrid assay

Directed Y2H experiments were performed with Clontech matchmaker GAL4 System following the manufacturer's recommendations. Briefly, AH109 yeast cells were co-transformed (Gietz & Schiestl, 1994) with the following pairwise construct combinations: pGADT7-AgT (SV40 large T antigen) + pGBKT7-p53 (tumor suppressor p53) and pGADT7-CP + pGBKT7-CP as positive controls; pGADT7-AgT + pGBKT7-lamC (laminin C) as the negative control; pGADT7-CP + pGBKT7-lamC and pGADT7-AgT + pGBKT7-CP as CP transcription autoactivation controls; pGADT7-AgT + pGBKT7-SlGSTUs as SlGSTUs transcription autoactivation controls; and finally pGADT7-CP + pGBKT7-SlGSTUs. Co-transformed yeast cultures were incubated with constant stirring at 30°C o/n, and next day they were serially diluted to 1 : 10, 1 : 100 and 1 : 1000. Three microlitres drops of each dilution from each culture were placed in co-transformation medium agar plates (SD−Leu/−Trp) and in selective media agar plates (SD−Leu/−Trp/−His, SD−Leu/−Trp/−His/ + 2 mM 3-AT, and SD−Leu/−Trp/−His/−Ade) and incubated at 30°C. Yeast growth was checked 2–3 d after.

Co-immunoprecipitation assay and immunoblot analysis

For the co-immunoprecipitation (CoIP) assay, three leaves of 5 *N. benthamiana* plants were syringe-agroinfiltrated (Ruiz-Ramón *et al.*, 2019) to express P19 (the tomato bushy stunt virus P19 RNA silencing suppressor) with the CP plus free GFP or GFP-SlGSTU38. Six disks from each infiltrated leaf were harvested for protein extraction with RIPA buffer (10 mM Tris–HCl pH 7.5, 150 mM NaCl, 0.5 mM EDTA, 0.1% SDS, 1% Triton X-100, 1% deoxycholate) supplemented with protease cocktail inhibitor (Roche) and DNaseI (Roche). The protein extracts were used as the input for CoIP using green fluorescent protein (GFP)-Trap® Agarose and spin columns (Chromotek, Planegg, Germany) following the manufacturer's indications. For the immunoblot analysis, inputs and bound fractions premixed with 5× Laemmli loading buffer (300 mM Tris–HCl pH 6.8, 50% Glycerol, 10% SDS; 0.05% bromophenol blue, 5% 2-mercaptoethanol) were loaded in a 12% SDS-PAGE gel and tank-electrotransferred to nitrocellulose membranes (Amersham Biosciences, Buckinghamshire, UK). Blots were probed for: CP detection with a polyclonal antibody raised in rabbit (AC Diagnostics Inc., Fayetteville, AR, USA); and for the GFP and GFP fusion proteins detection with an anti-GFP-monoclonal antibody raised in rat (Chromotek). The primary antibodies were detected by anti-rabbit or anti-rat immunoglobulin G (IgG) coupled to horseradish peroxidase (Promega) and chemiluminescent (ECL) substrate (SuperSignal West Femto Chemiluminescent Substrate; Thermo Fisher Scientific, Waltham, MA, USA).

Tomato transformation for *SlGSTU38* CRISPR/Cas9 editing

GV3101 *A. tumefaciens* cells transformed with pA60-GST19 were used for Micro-Tom transformation following a previously described method (Eck *et al.*, 2006). Four plants from two lines of T0 plants with WT phenotype were transferred to soil in pots and acclimatized in growth chamber. Mutations in *SlGSTU38* were identified in T1 generations using Phire Tissue direct PCR (Thermo Fisher Scientific). Biallelic edited plants with a premature stop codon next to the PAM sequence were selected, and T2 generation seeds were obtained. Then, the T2 progeny was analyzed by PCR to select individual plants that had lost the transgene. Seeds from plants not bearing the transgene were collected and multiplied for further experiments.

PepMV, TMV, and PVX susceptibility assays

The first two true leaves of 3-wk-old *SlGSTU38*-knocked-out plants (*gstu38*) and WT plants were mechanically inoculated with 10 µl each of 0.1 µg µl^{-1} PepMV virion prepared as in Agirrezabala *et al.* (2015), or with homogenates from *N. benthamiana* leaves systemically infected with TMV or PVX ground in 30 mM phosphate buffer pH 8.0. At 7 or 14-d postinoculation (dpi), the upper noninoculated Micro-Tom leaves were harvested individually from each plant, and total RNA was extracted with TRI reagent (Molecular Research Center Inc.) followed by phenol–chloroform purification and RNA ethanol precipitation. Then, RNAs were treated with DNaseI (Sigma Aldrich), quantified using a NanoDrop One (Thermo Fisher Scientific), and normalized, and RNA integrity was checked by agarose gel electrophoresis. Finally, the PepMV absolute quantitation from each RNA preparation was carried out with the one-step NZYSpeedy RT-qPCR Green, ROX plus kit (NZYTech) following the manufacturer's indication and using the primers CE2651 and CE2652 (Table S1) and a standard curve obtained from 1 : 10 serial dilutions of a 5 ng µl^{-1} PepMV-disassembled RNA stock. TMV and PVX were quantified by relative RT-qPCR (NZYTech, Lisbon, Portugal) using the 25S ribosomal RNA (25S) and the elongation factor 1-alpha (eEF1a) as housekeeping RNAs. We used primers CE2415 and CE2416 for the 25S amplification and CE1199 and CE1200 for the eEF1a (Table S1).

Protoplast isolation and PepMV inoculation

Micro-Tom protoplasts were isolated as described by Nieto *et al.* (2011). Three million protoplasts were resuspended in 300 µl of LAV0.5 (1× Murashige & Skoog medium, 0.51 mM MES, 0.1 M Glycine, 0.4 M Mannitol, pH adjusted to 5.7), mixed with 75 µg of PepMV virion in a 1.1 vol of PEG-Ca (30% PEG-4000, 0.4 M Mannitol pH 5.7, 0.3 mM $CaCl_2$), and incubated at room temperature for 6 min. Then, 4.4 vol. of W5 (2 mM MES pH 5.7, 5 mM KCl, 125 mM $CaCl_2$, 150 mM NaCl) were slowly added to the mixture, centrifuged at 100 ***g*** for 1 min, after which the supernatant was discarded. Protoplasts were washed with 8 ml of LAV0.5, precipitated by centrifugation at 200 ***g*** for 3 min, and resuspended in 2.5 ml of LAV0.5. The protoplast suspension was transferred to a glass Petri dish, and the time $t = 0$ was sampled immediately. Then, protoplasts were incubated at 25°C and constant light for 20–22 h, after which time $t = 1$ was sampled. After sampling, protoplasts were precipitated by centrifugation at 250 ***g*** for 3 min and resuspended in TRI reagent (Molecular Research Center Inc.) for total RNA extraction as described previously. PepMV quantification was carried out by relative RT-qPCR using the 25S ribosomal RNA as a housekeeping RNA.

Live-cell confocal imaging

The localization of fluorescent protein (FP) fusions was carried out using *N. benthamiana* as the experimental host. FP fusion proteins and PepGFPm2 (Ruiz-Ramón *et al.*, 2019) were transiently expressed together with P19 in *N. benthamiana* leaves by syringe agroinfiltration (Ruiz-Ramón *et al.*, 2019) at OD_{600} of 0.25, 0.2, and 0.1, respectively. Sections of agroinoculated *N. benthamiana* leaves at 3–5-d postagroinfiltration were infiltrated with water (to avoid bubble formation when observing under the microscope) and mounted onto glass microscope slides using double-sided tape and covered with a #1.5 cover glass (Duran Group Inc., Mainz, Germany) adding a small drop of water between the sample and the cover. All the images were taken in a Leica SP8 confocal laser scanning microscope with a glycerol-dipping ×63 lens (Leica, Wetzlar, Germany). The excitation wavelengths used were as follows: 488 nm for GFP and 561 nm for monomeric red fluorescent protein (mRFP). Detection ranges were optimized for each FP, and sequential scanning was used when co-localizing GFP and mRFP fusion proteins. The Microscope and Hybrid detectors (Leica) settings were adjusted for each individual image for optimizing the contrast. Images were collected using LasX software (Leica), and if necessary, the maximum projection tool was used.

RNA sequencing and data analysis

Three bulks per treatment of three normalized RNA extracts from individual mock-inoculated and PepMV-infected WT and *gstu38* plants from the PepMV-susceptibility assay at 7 dpi were prepared for RNA sequencing (RNA-seq). RNA-seq libraries were generated using the TrueSeq Stranded mRNA LT kit protocol with ribosomal depletion using Ribo-Zero plant kit (Illumina, San Diego, CA, USA). RNA-seq libraries were sequenced using the Illumina Novaseq 6000 platform (Macrogen Inc., Seoul, South Korea) to obtain PE 150-bp reads. The bioinformatics pipeline was described previously (Alcaide *et al.*, 2022). Briefly, raw data quality was analyzed using the FastQC tool (Andrews, 2010), and low-quality reads (Phred < 30) and adapter traces were removed using Trimmomatic (Bolger *et al.*, 2014). Filtered reads were mapped against v.SL2.5 of the reference *Solanum lycopersicum* genome (https://solgenomics.net) (Fernandez-Pozo *et al.*, 2015) using the Mem algorithm of Bwa software (Li & Durbin, 2009), and mapping quality was analyzed using Qualimap bamqc (García-Alcalde *et al.*, 2012). The number of reads mapping to each mRNA (v.2.4 of gene annotations) was counted using the *FeatureCounts* function from the rsubread R package (Liao *et al.*, 2019). The Bioconductor package DESeq2 (Anders & Huber, 2010; Love *et al.*, 2014) was used to determine differentially expressed genes (DEGs) between pairwise comparisons. The combined list of DEGs represents the list of genes used in next steps. The relative level of expression per gene was calculated as normalized read counts to fragments per kilobase per million mapped reads (FPKM). Expressed genes were considered those DEGs with an FPKM value higher than 1 in at least one treatment. R functions *hClust* and *plot* were used to compute and draw the hierarchical clustering dendrogram of samples. prcomp and the factoextra package were used to compute and draw the principal component analysis (PCA) plot. The Venn diagram of expressed genes and the *GST* genes heatmap were drawn using the VennDiagram and the pheatmap R packages, respectively. We considered PepMV-specific genes as those for which the FPKM value in PepMV-infected WT or *gstu38* plants was at least twofold the value in mock-inoculated WT or *gstu38* plants, respectively, as described by Feng *et al.* (2017). Finally, PepMV-specific genes were clustered in $k = 12$ discrete clusters regarding their expression pattern per treatment using hclust. Manual inspection of gene functions of clusters 4 and 6 was performed using the predicted protein sequence from v.SL2.5 of the *Solanum lycopersicum* genome (https://solgenomics.net) of each gene, against the UniProt database (http://www.uniprot.org). To validate the RNA-seq data, the expression patterns of selected transcripts in the RNA bulks were analyzed by relative RT-qPCR using the one-step NZY Speedy RT-qPCR Green kit, ROX plus (NZYTech), and *eEF1a* as the housekeeping gene. We used primers CE3247/CE3248, CE3278/CE3279, CE3241/CE3242, CE3272/CE3273, and CE1199/CE1200 for the *Solyc09g092260.2*, *Solyc07g041730.2*, *Solyc02g089620.2*, *Solyc02g078150.2*, and *eEF1A* amplification, respectively (Table S1).

Peroxidase (POX) and GST activities, lipid peroxidation determination and histochemical detection of H_2O_2 and superoxide radicals ($O_2^{\bullet-}$)

The POX and GST activities, the extent of lipid peroxidation (by estimating malondialdehyde) and the histochemical staining of reactive oxygen species (ROS) in leaves were detected according to Díaz-Vivancos *et al.* (2008). The H_2O_2 detection was carried

out by endogenous POX-dependent *in situ* staining with 3,3-diaminobenzidine whereas $O_2^{\bullet-}$ detection was performed using nitro blue tetrazolium. Then, for both stainings, leaves were decolorized with 80% (v/v) ethanol and photographed under visible light.

Chlorophyll fluorescence

The chlorophyll fluorescence parameters quantum yield of PSII (Y(PSII)), photochemical quenching (qP), nonphotochemical quenching (NPQ and qN), and the electron transport rate (ETR) were determined using a Pulse-Modulated Chlorophyll Fluorescence Monitoring System (FMS2+ Hansatech). The chlorophyll fluorescence measurements were performed only at 14 dpi because at 7 dpi leaves were not big enough to properly accommodate the fluorometer clamp.

Results

Identification of a tomato glutathione *S*-transferase specifically interacting with the PepMV CP

In order to identify host proteins interacting with the PepMV CP, we carried out a Y2H screening of a cDNA normalized library prepared from leaves of healthy and PepMV-infected tomato plants at different infection times. SlGSTU38, a predicted GST belonging to the *tau* class (Islam *et al.*, 2017) and encoded by locus *Solyc09g011580* (ITAG release 2.40), was identified as a highly likely PepMV CP-interacting protein (Fig. S1).

The SlGSTU38-CP interaction was checked in a directed Y2H assay (Fig. 1a). A set of SlGSTU38 homologs was also included in this assay to analyze the specificity of the potential CP-SlGSTU38 interaction. The tomato GST *tau* class includes 57 members (Islam *et al.*, 2017). A BLASTp search in The Sol Genomics Network database (https://solgenomics.net) (Fernandez-Pozo *et al.*, 2015) using the SlGSTU38 protein sequence as query identified 25 homologs with an *e*-value below 1e-50 (Table S3). As the family is large, we selected SlGSTU29, SlGSTU35, SlGSTU36, SlGSTU37, SlGSTU39, and SlGSTU40 for this assay because of their phylogenetic proximity to SlGSTU38 (Fig. S2). All the yeast cultures grew on the double-dropout co-transformation medium, indicating they were correctly co-transformed (Fig. 1a). Only the positive controls and the co-transformant CP + SlGSTU38 were able to grow on the three interaction media (Fig. 1a). Negative controls and yeast cultures co-transformed with any of the SlGSTU38 homologs tested and the CP did not grow on any interaction media, confirming a very specific SlGSTU38-CP interaction in yeast.

We next used a CoIP assay to test whether the interaction between the CP and SlGSTU38 takes place in plant cells. The CP was expressed together with free GFP or SlGSTU38 fused to GFP in *N. benthamiana* leaves. Protein extracts were prepared from leaves and used as inputs for CoIP with a specific GFP-trap agarose. The inputs and the GFP immunoprecipitations were analyzed in western blots probed with antibodies against either GFP or PepMV CP. The CoIP assay showed that the CP specifically coeluted with the immunoprecipitated GFP-SlGSTU38, but was not detected in the bound fraction of the negative control (Fig. 1b), showing that the CP-SlGSTU38 interaction also takes place *in planta*.

SlGSTU38 is a PepMV-specific susceptibility factor with a cell-autonomous effect

SlGSTU38-knocked-out tomato cv Micro-Tom plants (*gstu38*) were generated by using the CRISPR/Cas9 technology. We designed a guide RNA (gRNA) targeting the *SlGSTU38* as close as possible to the 5′ end of the coding sequence, with no predicted off-targets, and with an optimal predicted folding when fused to the RNA scaffold (Liang *et al.*, 2016). We selected a line containing an insertion of one nucleotide next to the PAM sequence in homozygosis, leading to an early stop codon in the protein sequence (Fig. 2a). This early stop codon is expected to give rise to a truncated and nonfunctional SlGSTU38 protein of 64 amino acids. WT and *gstu38* Micro-Tom plants were inoculated with PepMV purified virions. All the leaves above the inoculated ones were harvested from each plant at 7 and 14 dpi, and the PepMV accumulation was quantified by absolute RT-qPCR. The PepMV accumulation in *gstu38* plants was significantly reduced compared with the WT plants at both sampling times (Fig. 2b). This result shows that SlGSTU38 has a proviral function for PepMV. *SlGSTU38*-knocked-out tomato plants showed no observable phenotype other than reduced susceptibility to PepMV (Fig. S3).

We next inoculated protoplasts isolated from leaves of WT or *gstu38* plants with PepMV virions and sampled them at 0 ($t = 0$) and 20–22 ($t = 1$) h postinoculation (hpi) for viral quantification. Inoculations of WT protoplasts with UV-inactivated PepMV virions were included as a negative control. For both genotypes, PepMV accumulation increased at $t = 1$ (Fig. 2c). However, PepMV accumulation was higher in WT than in *gstu38* protoplasts (Fig. 2c), suggesting that SlGSTU38 may have a cell-autonomous effect on PepMV accumulation.

To analyze whether SlGSTU38 is a PepMV-specific susceptibility factor or, by contrast, a factor involved in a general interaction with plant viruses, we challenged WT and *gstu38* Micro-Tom plants with either TMV or PVX. At 14 dpi, all the leaves above the inoculated ones were harvested from each plant individually for viral RNA quantification by relative RT-qPCR. No viral accumulation differences were observed in either TMV or PVX-infected *gstu38* plants compared with WT plants (Fig. 3), suggesting that *gstu38* plants' resistance is PepMV-specific.

SlGSTU38 colocalizes with the PepMV CP within the viral replication complexes

The PepMV CP fused to mRFP was expressed in *N. benthamiana* leaves for live-cell localization of the CP. The fluorescent signal emitted by mRFP-CP was observed in epidermal leaf cells and localized mainly to the cytoplasm and also within the nucleus (Fig. S4a). The GFP-SlGSTU38 fusion protein was also independently expressed in *N. benthamiana* leaves. The fluorescent

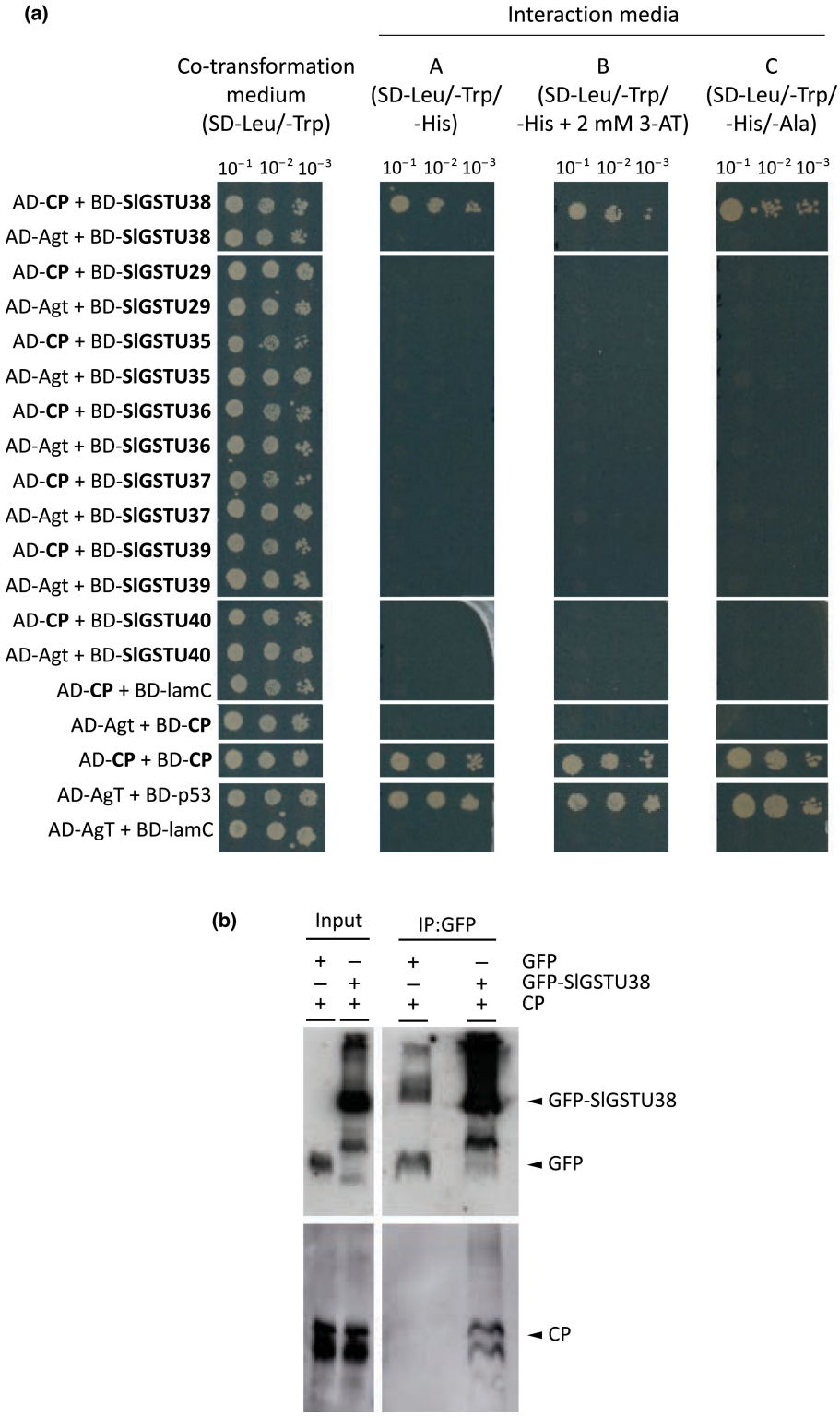

Fig. 1 Pepino mosaic virus (PepMV) coat protein (CP) interacts specifically with SlGSTU38 among the phylogenetically close SlGSTU38 homologs. (a) Directed yeast two-hybrid assay to validate CP-SlGSTU38 interaction including six phylogenetically close SlGSTU38 homologs. Three dilutions of co-transformed yeast cultures incubated on co-transformation medium (SD−Leu/−Trp) lacking leucine and tryptophan, and interaction media A, B, and C (arranged from least to most restrictive). Interaction medium A (SD−Leu/−Trp/−His) lacks leucine, tryptophan, and histidine. Interaction medium B (SD−Leu/−Trp/−His + 2 mM 3-AT) lacks leucine, tryptophan, and histidine and contains 2 mM of 3-amino-1,2,4-triazole (3-AT), a competitive inhibitor of the *HIS3* gene product. Interaction medium C (SD−Leu/−Trp/−His/−Ala) lacks leucine, tryptophan, histidine, and alanine. Yeast cultures coexpressing AD-AgT + BD-p53 and AD-CP + BD-CP were used as positive control. Pairs AD-AgT + BD-lamC, AD-CP + BD-lamC, AD-AgT + BD-CP, and AD-AgT + BD-SlGSTUs were negative controls. All the co-transformants were leucine and tryptophan autotrophs, since they grew on the co-transformation medium indicating they were correctly co-transformed. CP-SlGSTU38 and positive control interactions were visualized by yeast co-transformant growth in A, B, and C interaction media indicating *HIS3* and *ADE2* reporter gene activation. AD-AgT, Gal4 activation domain fused to the SV40 large T antigen. BD-p53, Gal4 binding domain fused to the murine p53. BD-lamC, Gal4 binding domain fused to laminin C. AD-CP, Gal4 activation domain fused to the CP. BD-SlGSTUs, Gal4 binding domain fused to SlGSTUs. (b) A co-immunoprecipitation assay confirmed the CP-SlGSTU38 *in planta* interaction. Protein extracts from *Nicotiana benthamiana* leaves expressing CP together with free GFP or GFP-SlGSTU38 were used as inputs for GFP immunoprecipitation (IP:GFP). Antibodies anti-CP and anti-GFP were used for western-blot detection of CP and GFP-SlGSTU38, respectively. The CP was copurified with the immunoprecipitated GFP-SlGSTU38.

signal emitted by GFP-SlGSTU38 was observed in the cytoplasm and the nucleus, as before for mRFP-CP (Fig. S4b). When both fusion proteins were co-expressed in *N. benthamiana* leaves, no subcellular relocalization of GFP-SlGSTU38 or mRFP-CP was observed, and both fusion protein signals strongly colocalized, suggesting that the CP and SlGSTU38 have the same subcellular distribution (Fig. S4c–h).

The PepGFPm2 agroinfectious clone (Ruiz-Ramón *et al.*, 2019) was used to analyze the subcellular localization of SlGSTU38 and CP during PepMV infection. PepGFPm2 expresses GFP through a translational fusion to the N terminus of the CP, *via* the 2A peptide of the foot-and-mouth disease virus (Fig. 4a) (Ruiz-Ramón *et al.*, 2019). When PepGFPm2 and mRFP-SlGSTU38 were co-expressed in *N.*

New Phytologist

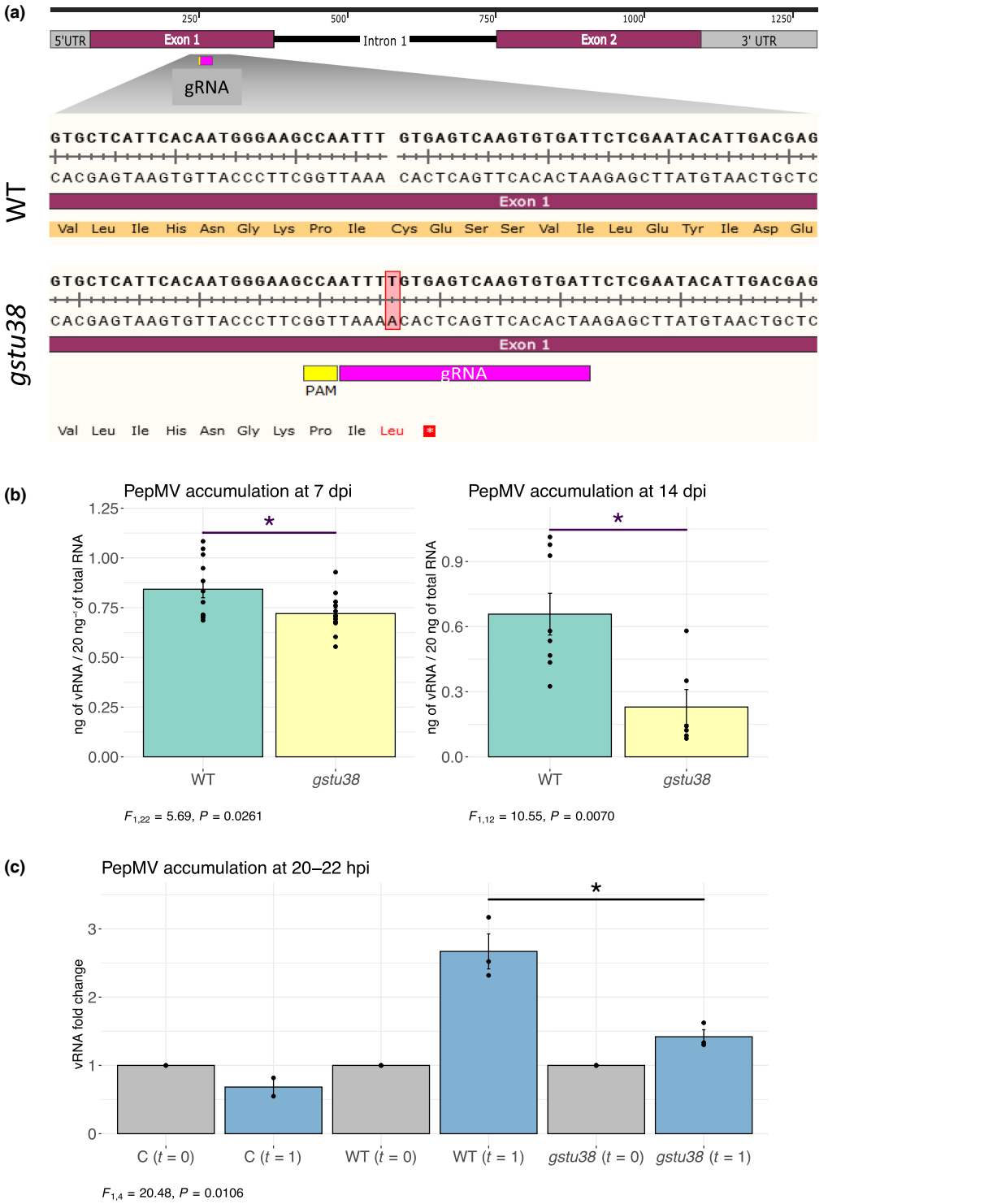

Fig. 2 Pepino mosaic virus (PepMV) multiplication is reduced in *SlGSTU38*-knocked-out plants in a cell-autonomous manner. (a) The CRISPR/Cas9 technology was used to knock out *SlGSTU38*. In the upper part of the panel, the *SlGSTU38* gene and the relative position of the guide RNA (gRNA) target are represented. In the lower part of the panel, results of the genotyping of a wild-type Micro-Tom plant (WT) and a *SlGSTU38* edited Micro-Tom plant (*gstu38*) are shown; a single-nucleotide insertion (in red) in homozygosis was detected in *gstu38* plants. The putative protein sequence is also shown; a red square represents a premature stop codon. (b) PepMV accumulation is reduced in SlGSTU38-knocked-out plants. Bar plots show the absolute accumulation of PepMV RNA (ng per 20 ng of total RNA) in WT and *gstu38* PepMV-infected plants at 7- and 14-d postinoculation (dpi). Error bars represent the SE. Asterisks indicate statistically significant differences between groups computed by one-way ANOVA (7 dpi: $F_{1,22} = 5.69$, $P = 0.0261$; 14 dpi: $F_{1,12} = 10.55$, $P = 0.0070$). (c) PepMV multiplication is reduced in protoplasts isolated from SlGSTU38-knocked-out plants. Bar plot shows the PepMV viral RNA (vRNA) fold change at 20–22 ($t = 1$) h postinoculation (hpi) in PepMV-inoculated protoplasts isolated from leaves of WT or *gstu38* plants compared with the PepMV relative accumulation at 0 hpi ($t = 0$). Incubation of WT protoplasts inoculated with UV-inactivated PepMV virions was included as negative control (C−). Error bars represent the SE. An asterisk indicates statistically significant differences between groups computed by one-way ANOVA ($F_{1,4} = 20.48$, $P = 0.0106$).

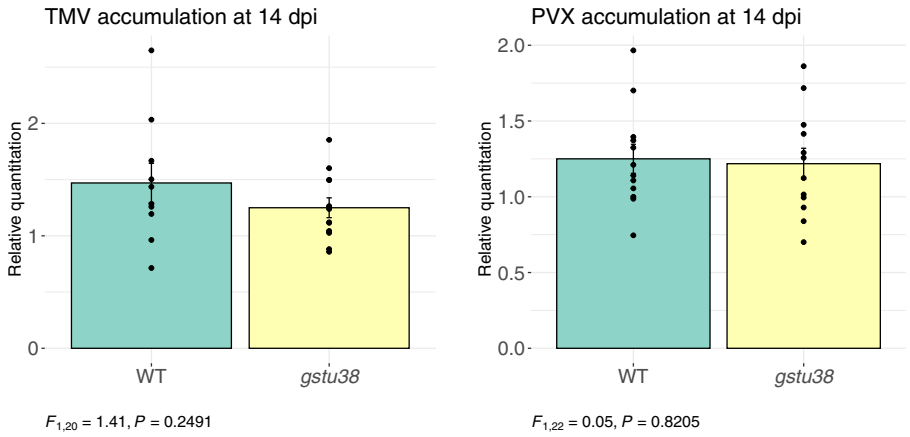

Fig. 3 Tobacco mosaic virus (TMV) and potato virus X (PVX) are not affected in *SlGSTU38*-knocked-out plants. Bar plots show the TMV or PVX relative quantification in wild-type (WT) and *gstu38* infected plants at 14-d postinoculation (dpi). Error bars represent the SE. No statistically significant differences were observed between groups by one-way ANOVA (TMV: $F_{1,20} = 1.41$, $P = 0.2491$) (PVX: $F_{1,22} = 0.05$, $P = 0.8205$).

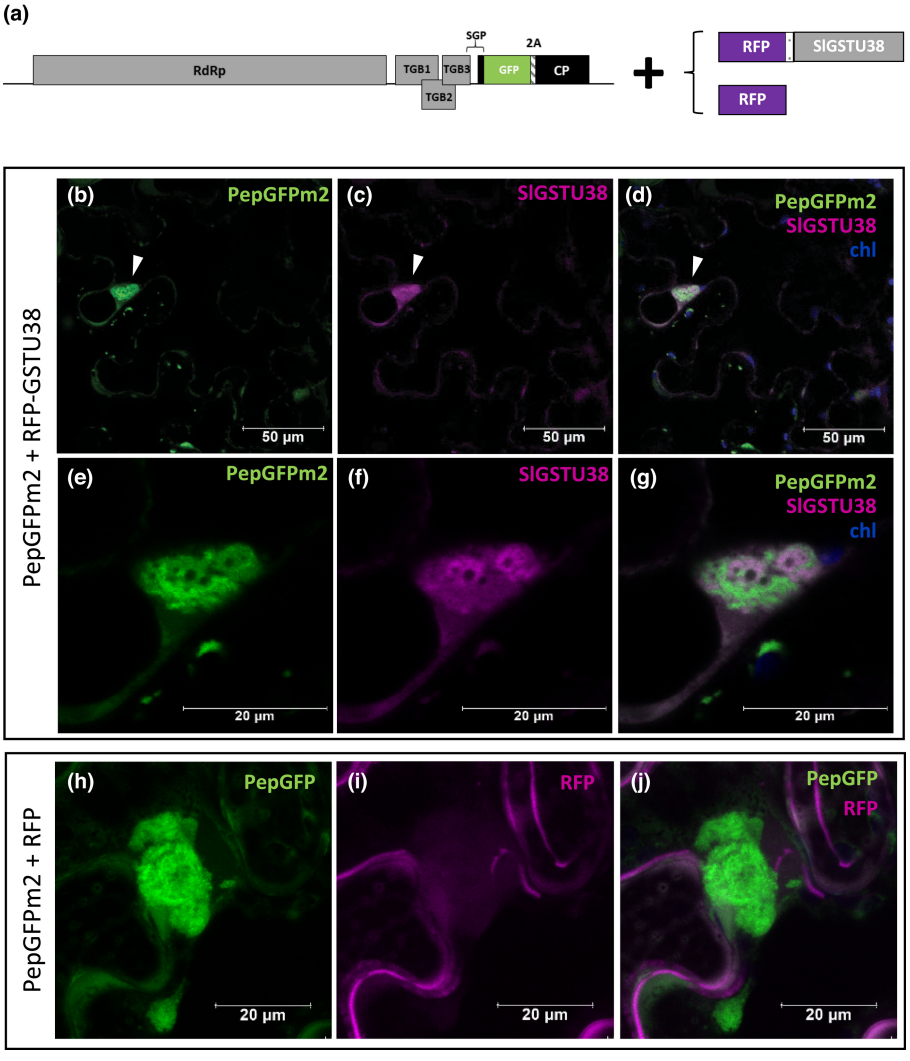

Fig. 4 SlGSTU38 localizes within the Pepino mosaic virus (PepMV) replication complex. (a) Schematic representation of the genomic organization of PepGFPm2 (Ruiz-Ramón *et al*., 2019), and its coexpression with mRFP-SlGSTU38 or free mRFP. PepGFPm2 expresses GFP fused to the CP *via* the 2A peptide. RdRp, RNA-dependent RNA polymerase; TGB1, 2 and 3, Triple gene block 1, 2, and 3 protein-encoding genes; SGP, subgenomic promoter; 2A, foot-and-mouth disease virus 2A peptide; CP, coat protein. (b–g) GFP and mRFP channels, and the overlay with the chloroplast autofluorescence (chl) from an image of a cell expressing both PepGFPm2 and mRFP-SlGSTU38. An arrowhead indicates a viral replication complex (VRC). (e–g) Magnification of the VRC. (h–j) GFP and mRFP channels, and the overlay of a maximum projection of a Z-stack of a VRC in a cell expressing PepGFPm2 and free mRFP.

benthamiana leaves, mRFP-SlGSTU38 colocalized with the GFP-CP within the VRCs (Fig. 4b–g). As a negative control, PepGFPm2 and free mRFP were co-expressed, and only a weak mRFP signal was observed within the PepMV VRCs (Fig. 4h–j), suggesting a specific relocalization of SlGSTU38 to the PepMV VRCs.

SlGSTU38 knock-out deregulates stress-responsive genes

WT and *gstu38* plants, both healthy and PepMV-infected, were analyzed by RNA-seq. We used total RNA from the PepMV-susceptibility assay at 7 dpi described previously and total RNA from mock-inoculated WT and *gstu38* plants grown at the same

time in the same chamber as healthy plants. We constructed three independent RNA-seq libraries per genotype and per treatment. RNA-seq libraries were subjected to high-throughput sequencing using the Illumina platform. After filtering by quality and mapping reads against the tomato genome, read counts were normalized to fragments per kilobase per million mapped reads (FPKM) and genes with an FPKM higher than 1 in at least one treatment were considered as expressed genes. The three

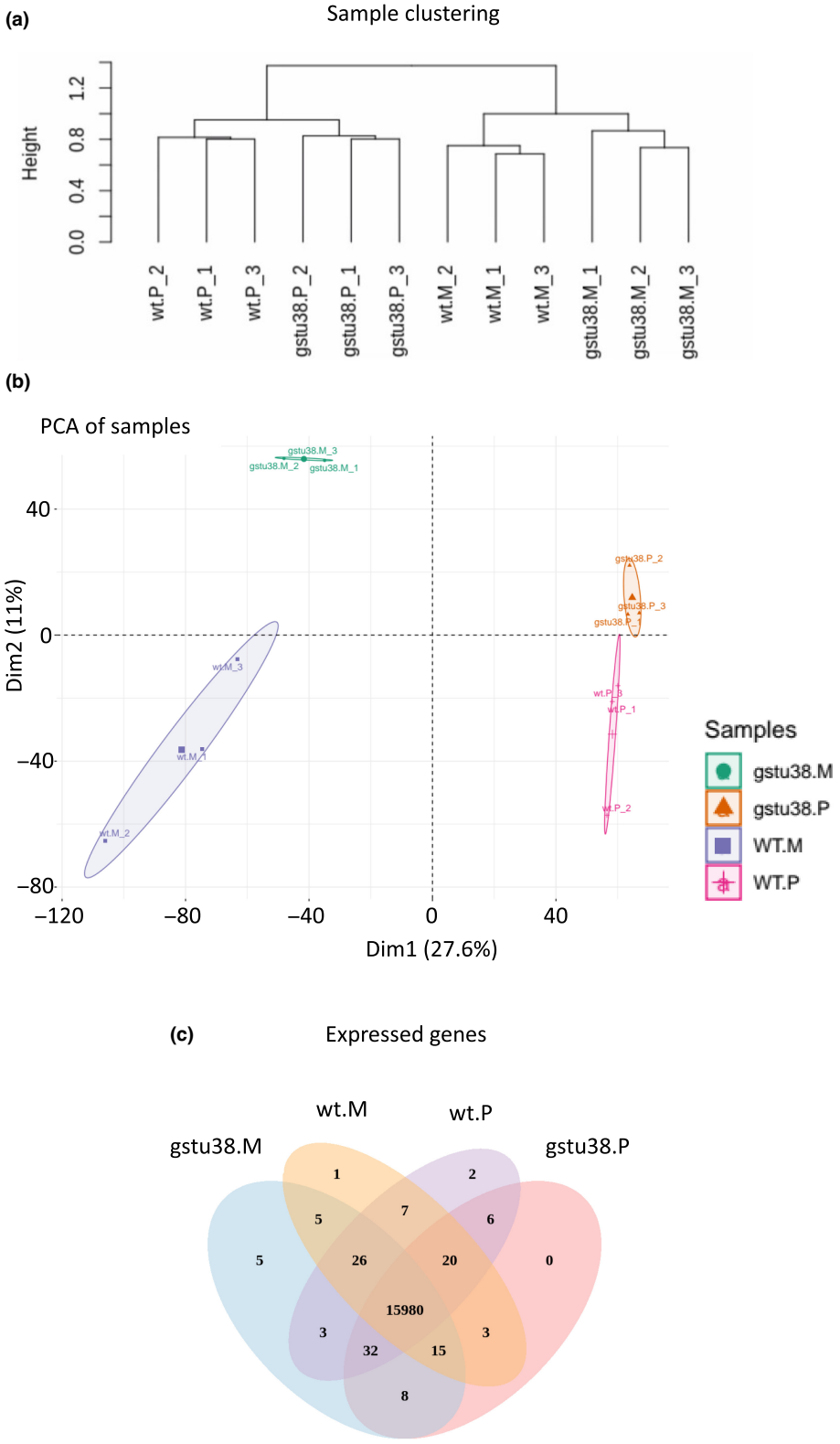

Fig. 5 RNA-seq of healthy and Pepino mosaic virus (PepMV)-infected wild-type (WT) and gstu38 Micro-tom plants at 7-d postinoculation. (a) Cluster dendrogram of gene expression profiles between biological replicates of healthy (M) and PepMV-infected (P) WT and *gstu38* plants. The dendrogram shows the hierarchical clustering of the replicates according to their gene expression profiles. (b) Principal component analysis (PCA) scores plotted for healthy (M) and PepMV-infected (P) WT and *gstu38* plants. The PCA was computed using expressed genes. The percentage of variance explained by dimension 1 (Dim1) and 2 (Dim2) are 26.6% and 11%, respectively. Confidence ellipses were plotted around group mean points. (c) Venn diagrams showing the numbers of expressed genes specific to or shared among plants from different genotypes and treatments. Venn diagrams were drawn using expressed genes.

biological replicates from each treatment clustered together in a clustering analysis (Fig. 5a) and assembled together in a PCA (Fig. 5b). The PCA also showed differentiation between healthy and infected plants and between genotypes (Fig. 5b). The number of expressed genes was around 16 000 for each treatment (Table S4). A Venn diagram of expressed genes (Fig. 5c) showed that most of them (15 980) were expressed in all treatments, and only five, one, and two genes, mostly encoding putative proteins of unknown function, were exclusively expressed in mock-inoculated *gstu38*, mock-inoculated WT, and PepMV-inoculated WT plants, respectively (Table S5). We next identified the DEGs for all the possible pairwise comparisons between treatments (Table S6). Out of 154 DEGs in the comparison *gstu38* vs WT healthy plants, 129 were upregulated and 25 were downregulated. No gene ontology (GO) categories were found to be significantly overrepresented, but a manual inspection of the DEGs revealed an important number of stress-related genes upregulated for this comparison (Table S7), including *SlGSTU36*, *SlGSTU43*, *SlGSTU51*, and the genes encoding three PEROXIDASES, one CALMODULIN-LIKE PROTEIN, one MILDEW RESISTANCE LOCUS O (MLO)-LIKE PROTEIN, two GELSOLINS, one CALRETICULIN 2 calcium-binding protein, one CAFFEOYL-CoA O-METHYLTRANSFERASE, two GLUTAMATE RECEPTOR-LIKE PROTEINS, 21 RECEPTOR PROTEIN KINASES, four NUCLEOTIDE BINDING SITE/LEUCINE-RICH REPEAT (NBS-LRR) proteins, and five WRKY TRANSCRIPTION FACTORS, among others (Table S7). Downregulated genes in *gstu38* vs WT healthy plants were more diverse and included four genes encoding proteins that participate in intracellular signal transduction, four genes encoding transcription factors (a CONSTANS-LIKE ZINC FINGER PROTEIN, a NAC DOMAIN PROTEIN, a B3 DOMAIN-CONTAINING TRANSCRIPTION FACTOR VRN1 and a CCR4-NOT TRANSCRIPTION COMPLEX subunit 7), two HEAT SHOCK PROTEIN 70 (HSP70), and three genes encoding proteins involved in sugar metabolism or transport, among others (Table S7).

The expression of all the *GST* genes (Islam *et al.*, 2017) in healthy and PepMV-infected WT plants was analyzed using a heatmap of FPKM values. The *SlGSTU38* gene was one of the most expressed *GST* genes in both healthy and infected WT plants and was not inducible by PepMV infection (Fig. 6). Close homologs of *SlGSTU38* were not expressed or expressed at low levels in both healthy and infected WT plants (Fig. 6).

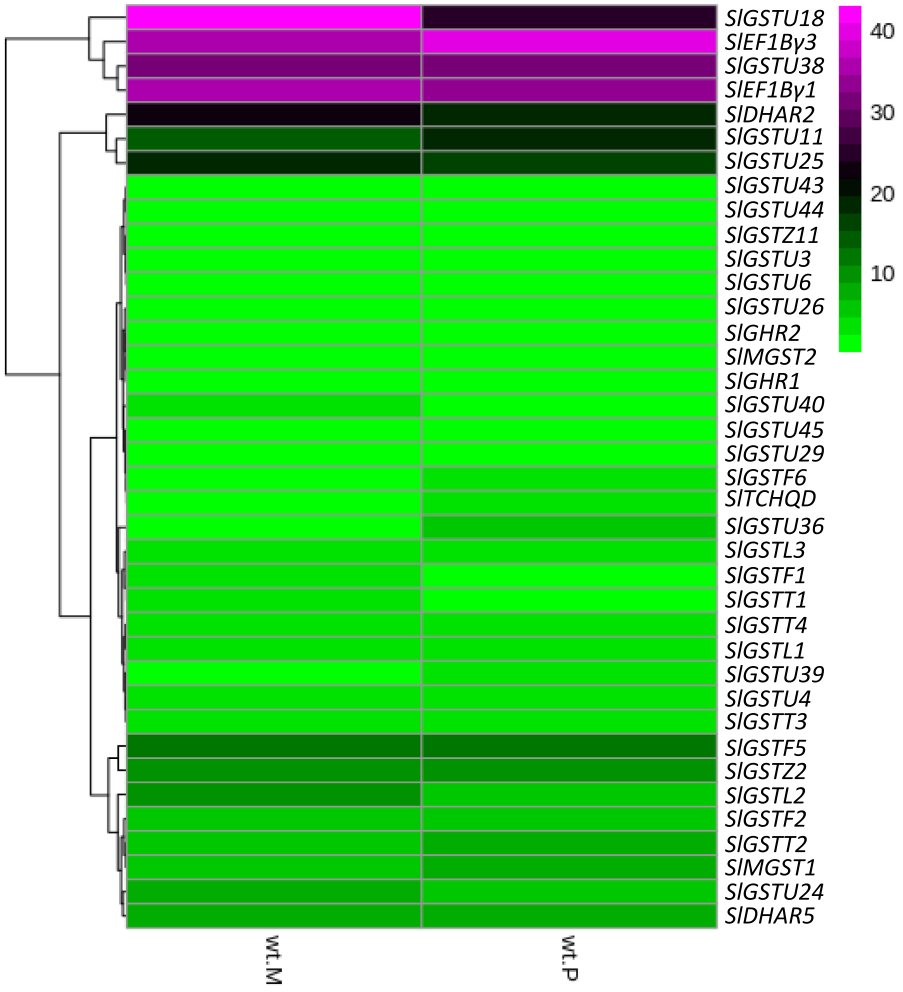

Fig. 6 *SlGSTU38* is among the most expressed *GST* genes in both healthy and Pepino mosaic virus (PepMV)-infected wild-type (WT) plants. Heatmap of *GST* genes that are expressed in healthy (wt.M) or PepMV-infected (wt.P) WT plants. Scaled fragments per kilobase per million mapped reads (FPKM) values were used as input and are represented by colors. Lower to higher expression is represented by bright green to bright magenta.

There is a large difference in genes deregulated by PepMV in *gstu38* vs wild-type plants

A total of 789 genes were deregulated by PepMV infection. Among these, 220 genes were shared by plants of both genotypes, whereas 392 genes were specifically deregulated in WT and 177 genes in *gstu38* plants. The 789 PepMV-specific DEGs were grouped into 12 clusters according to their expression patterns in the different treatments (Fig. 7). A further inspection was carried out with genes of clusters 4 and 6; cluster 4 groups genes downregulated in *gstu38* plants but upregulated in WT plants during PepMV infection, and cluster 6 includes genes specifically upregulated in PepMV-infected *gstu38* plants (Fig. 7). In clusters 4 and 6, we found 16 and 14 genes, respectively (Table 1). Cluster 4 included genes encoding a peroxidase, an LRRNT_2 DOMAIN-CONTAINING PROTEIN, a PROTEIN KINASE DOMAIN-CONTAINING PROTEIN; an RNA RECOGNITION MOTIF DOMAIN-CONTAINING PROTEIN, a CC-NBS-LRR resistance protein, and a THAUMATIN-LIKE PROTEIN, among others (Table 1). Cluster 6 included genes encoding a GATA TRANSCRIPTION FACTOR, a GIBBERELLIN-REGULATED PROTEIN, a PROLINE DEHYDROGENASE, two proteins positively regulated by ABA signaling (a GEM-LIKE PROTEIN and MOB1A), the DNA REPAIR AND RECOMBINATION PROTEIN RAD54, a transcription activator predicted as a growth-regulating factor, a chaperone protein DNAJC, and a HAIRPIN-INDUCED PROTEIN-LIKE (HIN1) PROTEIN, among others (Table 1). Transcripts from *Solyc09g092260.2*, *Solyc07g041730.2*, *Solyc02g089620.2*, *and Solyc02g078150.2* (Table 1) were quantified by relative RT-qPCR for each treatment, validating the RNA-seq data (Fig. S5).

SlGSTU38 is involved in the cellular redox homeostasis

We hypothesized that SlGSTU38 may be involved in the cellular redox homeostasis. Superoxide ($O_2^{\bullet-}$) and hydrogen peroxide (H_2O_2) accumulation in leaves from healthy and PepMV-infected WT and *gstu38* plants at 7 and 14 dpi were detected by histochemical staining with nitro blue tetrazolium (NBT) and diaminobenzidine (DAB), respectively. No $O_2^{\bullet-}$ accumulation was detected for any of the treatments at 7 dpi other than small isolated dots (Fig. 8a). At 14 dpi, $O_2^{\bullet-}$ accumulation was observed in healthy *gstu38* leaves and in PepMV-infected leaves from both WT and *gstu38* genotypes (Fig. 8a). The DAB staining showed H_2O_2 accumulation in healthy and PepMV-infected *gstu38* leaves at 7 dpi, while lower H_2O_2 accumulation was observed in WT leaves (Fig. 8a). At 14 dpi, PepMV strongly induced H_2O_2 production in both genotypes, and we observed again more H_2O_2 accumulation in healthy *gstu38* leaves than in healthy WT leaves (Fig. 8a). These results indicate that both PepMV and SlGSTU38 knockout induce $O_2^{\bullet-}$ and H_2O_2 accumulation. DAB staining results appeared to correlate with the POX activity data for each treatment. PepMV infection had an effect on POX activity in WT but not in *gstu38* plants at any of the postinoculation times (Fig. 8b). Regarding the GST activity, we observed a significant decrease induced by PepMV infection in WT plants at 7 and 14 dpi, while no effect was observed in *gstu38* plants (Fig. 8b). Moreover, in the absence of PepMV infection, a slight but nonsignificant decrease in GST activity was recorded in *gstu38* compared with WT (Fig. 8b). These results indicate that PepMV infection increases POX activity and decreases GST activity in WT plants, while SlGSTU38 knockout enhances POX activity but both POX and GST activities remain unaffected after PepMV infection. We then measured lipid peroxidation as an oxidative stress marker and no differences between treatments were observed (Fig. S6), suggesting that PepMV or SlGSTU38 knockout are not inducing a severe oxidative stress even though some ROS accumulation occurred (Fig. 8a). PepMV infection and SlGSTU38 knockout associated with an increase in nonphotochemical chlorophyll fluorescence quenching parameters (qNP and NPQ; Fig. 8c), which are related with the harmless dissipation of excess energy as heat. In addition, SlGSTU38 knockout decreased the photosynthetic electron transport chain (ETR) activity compared with the WT plants, whereas PepMV increased ETR *c.* 7% and 12% in WT and *gstu38*, respectively, reaching similar values in both genotypes (Fig. 8c).

Discussion

In this work, we demonstrated that PepMV CP interacts with tomato SlGSTU38. Three lines of evidence support a functional role for SlGSTU38 in the PepMV infectious cycle: (1) PepMV CP specifically interacts with SlGSTU38 among phylogenetically close GSTs (Fig. 1); (2) knockout *SlGSTU38* in tomato leads to partial loss of susceptibility to PepMV (Fig. 2b) in a cell-autonomous way (Fig. 2c); and (3) SlGSTU38 accumulates in the PepMV VRC (Fig. 4). Moreover, knocking out *SlGSTU38* upregulates stress and pathogen responsive genes and increases ROS accumulation and POX activity suggesting a role of SlGSTU38 in the cellular redox homeostasis. We propose here that SlGSTU38 may have a double involvement in PepMV infection: A direct participation depending on the interaction with the CP and an indirect participation maintaining the cellular homeostasis and delaying PepMV infection sensing and the plant defense response. The combination of both phenomena may explain why *gstu38* plants, despite having their innate immune responses apparently activated, did not show loss of susceptibility to the other two viruses tested (Fig. 3).

PepMV, just as other potexviruses, recruits ER membranes to form its VRCs (Tilsner *et al.*, 2012; Ruiz-Ramón *et al.*, 2019). The ER lumen is a unique and oxidative environment. GSTs are antioxidant proteins and NbGSTU4 has been described as a susceptibility factor interacting with the 3′UTR of the BaMV genome and reducing conditions seem to be required for optimal BaMV minus-strand RNA synthesis (Chen *et al.*, 2013). In this work, we demonstrated the VRC localization of SlGSTU38 (Fig. 4). We also observed a decrease in PepMV accumulation in *gstu38* plants and protoplasts, indicating that SlGSTU38 is likely directly involved in virus cellular functions (Fig. 2b,c). We propose that PepMV CP interacts with and recruits SlGSTU38 to the VRC to generate optimal redox conditions for virus

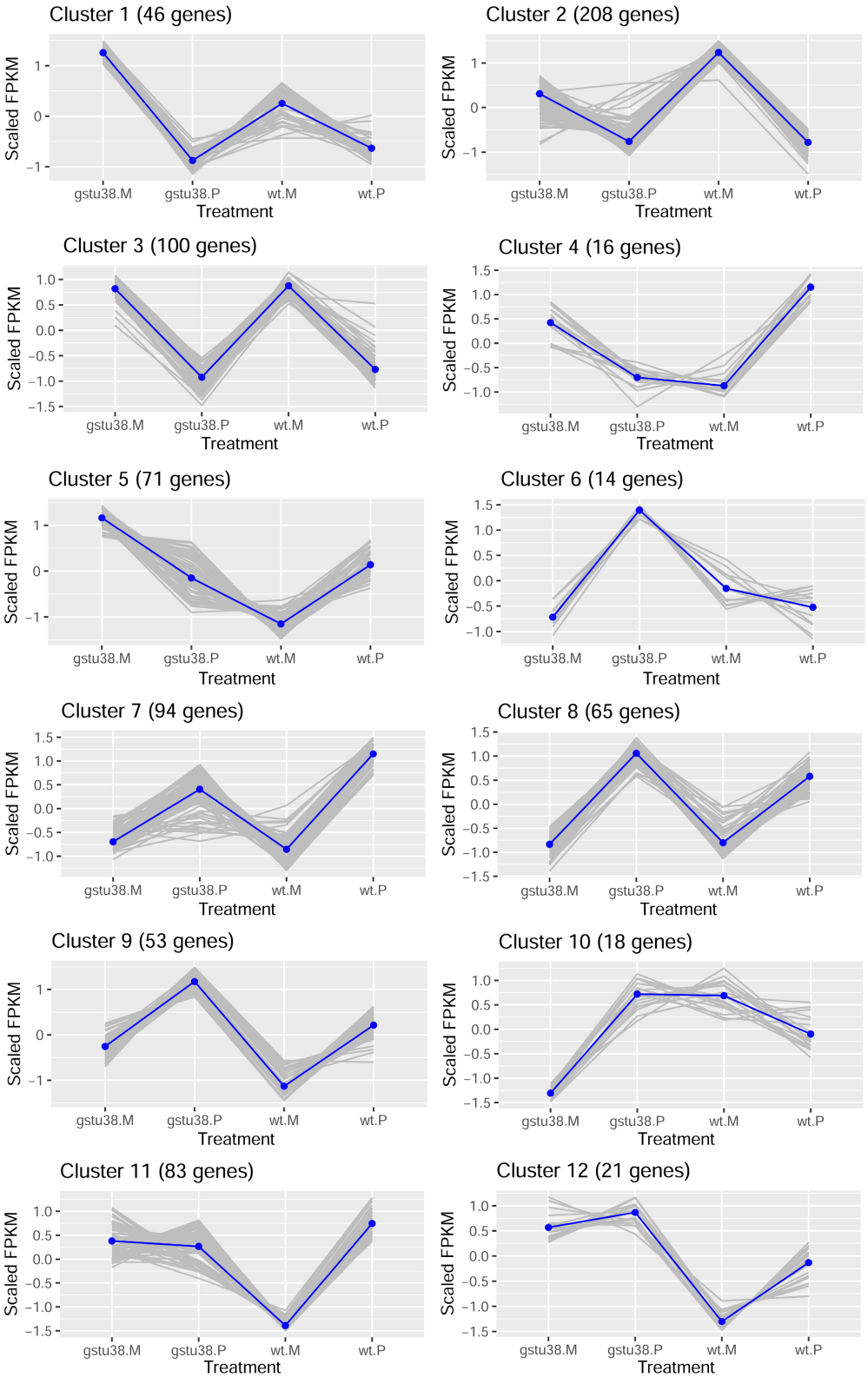

Fig. 7 Expression patterns of differentially expressed genes (DEGs) in wild-type (WT) and *gstu38* genotypes. Scaled fragments per kilobase per million mapped reads (FPKM) values of Pepino mosaic virus (PepMV)-specific DEGs (789) were used for hierarchical gene clustering by calculating the distances of the Pearson correlations of one gene to another. Discrete clusters were extracted setting $k = 12$. Gray lines represent the scaled FPKM values of each gene in each treatment. Blue lines represent the expression dynamic of each cluster calculated by the mean of scaled FPKM of genes included in each cluster for each treatment. Treatments were WT healthy (wt.M), WT infected with PepMV (wt.P), *gstu38* healthy (gstu38.M), and *gstu38* infected with PepMV (gstu38.P).

Table 1 ID and description of genes included in clusters 4 and 6.

	Gene ID	Gene description
Cluster 4	Solyc01g057680.2	LRRNT_2 DOMAIN-CONTAINING PROTEIN
	Solyc02g049090.1	UNKNOWN PROTEIN
	Solyc02g071560.2	SUBTILISIN-LIKE PROTEASE
	Solyc02g081040.2	PROTEIN KINASE DOMAIN-CONTAINING PROTEIN
	Solyc02g086980.2	UNKNOWN PROTEIN
	Solyc03g123750.2	LIPASE_3 DOMAIN-CONTAINING PROTEIN
	Solyc05g021530.1	UNCHARACTERIZED PROTEIN
	Solyc05g053780.2	RNA RECOGNITION MOTIF DOMAIN-CONTAINING PROTEIN
	Solyc07g055770.1	UNKNOWN PROTEIN
	Solyc07g065380.2	ZINC TRANSPORTER
	Solyc08g076850.2	SENESCENCE-ASSOCIATED PROTEIN
	Solyc09g007520.2	PEROXIDASE
	Solyc09g089940.1	UNCHARACTERIZED PROTEIN
	Solyc09g092300.2	CC-NBS, RESISTANCE PROTEIN FRAGMENT
	Solyc11g063510.1	UNCHARACTERIZED PROTEIN
	Solyc12g056360.1	THAUMATIN-LIKE PROTEIN
Cluster 6	Solyc00g007150.2	UNKNOWN PROTEIN
	Solyc01g060070.2	PORE PROTEIN HOMOLOG
	Solyc01g090760.2	GATA TRANSCRIPTION FACTOR
	Solyc02g078150.2	PLANT-SPECIFIC DOMAIN TIGR01615 FAMILY PROTEIN
	Solyc02g083880.2	GIBBERELLIN-REGULATED PROTEIN 2
	Solyc02g089620.2	PROLINE DEHYDROGENASE
	Solyc04g008930.1	GEM-LIKE PROTEIN
	Solyc04g056400.2	DNA REPAIR AND RECOMBINATION PROTEIN RAD54
	Solyc07g041730.2	MPS ONE BINDER KINASE ACTIVATOR-LIKE 1A (MOB1A)
	Solyc08g079800.2	GROWTH-REGULATING FACTOR 12
	Solyc09g092260.2	CHAPERONE PROTEIN DNAJ 20
	Solyc10g009230.1	UNKNOWN PROTEIN
	Solyc10g081980.1	HARPIN-INDUCED PROTEIN-LIKE PROTEIN
	Solyc11g040030.1	HISTIDINOL-PHOSPHATE AMINOTRANSFERASE

In orange, genes from cluster 4 encoding proteins predicted to have immune response functions. In green or blue, genes from cluster 6 positively regulated in abscisic acid or salicylic acid signaling pathways, respectively.

replication. The decrease in PepMV accumulation in *gstu38* plants and protoplasts may occur because of suboptimal conditions of the redox balance within the VRCs. Moreover, the *SlGSTU38* transcript is constitutively expressed in tomato plants and accumulates at higher levels than the transcripts of its homologs (Fig. 6), implying that PepMV may have abundant SlGSTU38 from early infection, regardless of transcriptomic reprogramming and without any temporal delay. It would therefore also make sense for the virus to have evolved to interact with this particular abundant GST isoform (Huang *et al.*, 2012).

SlGSTU38 has constitutive expression and its knockout induces ROS accumulation in leaves (Fig. 8), indicating that SlGSTU38 is involved in the cellular redox homeostasis under normal conditions. We propose that *SlGSTU38* knockout induces a disruption of the redox homeostasis, triggering the activation of stress and pathogen responses in healthy plants and leading to early PepMV-sensing by the plant and delaying infection. In this sense, the stress acclimation mechanism has been related to the electron transfer chain (ETC) since electrons supply may be needed to support the defense responses (Karpiński *et al.*, 2013; Moreau *et al.*, 2020), and the observed induction of the ETR in PepMV-infected *gstu38* plants may trigger and modulate the defense responses (Fig. 8). SlGSTU38 absence in mutant plants induced the upregulation of genes encoding three GSTs (SlGSTU36, SlGSTU43, and SlGSTU51) and three peroxidases. This correlated with enhanced POX and unaffected GST activities in *gstu38* vs WT healthy plants (Fig. 8), suggesting a compensatory antioxidative response. PepMV infection also increased POX activity but decreased GST activity in WT plants, as similarly described for plum pox virus infection in pea plants (Díaz-Vivancos *et al.*, 2008). Our transcriptomic analysis also suggests calcium-signaling activation in *gstu38* plants (Table S7, genes marked in blue), reinforcing the idea of constitutive and systemic activation of a stress response in those plants. Also, ethylene and abscisic acid (ABA)-signaling pathways may be activated in *gstu38* plants (Table S7, genes marked in green and purple). Both ABA and ethylene play essential roles in the response to a variety of abiotic stresses (Vishwakarma *et al.*, 2017; Husain *et al.*, 2020; Riyazuddin *et al.*, 2020), and the redox state is a key modulator of defense responses including phytohormone biosynthesis and crosstalk (Bartoli *et al.*, 2013; Kocsy *et al.*, 2013). SlGSTU38 absence also induced the upregulation of 39 genes encoding proteins involved in signal transduction (Table S7, genes marked in yellow), including 18 proteins containing the LEUCINE-RICH REPEAT domain, which is related to pathogen sensing and other biotic or abiotic stimuli (Padmanabhan *et al.*, 2009). Another 13 genes encoding proteins predicted by homology to be related to abiotic and/or biotic stresses were upregulated in *gstu38* plants (Table S7, genes marked in orange). Interestingly, two genes encoding HSP70 isoforms were downregulated in *gstu38* plants, with one of them (HSC70.3) already described as a PepMV-susceptibility factor and a PepMV CP interactor (Mathioudakis *et al.*, 2012, 2014). The Hsc70.3 downregulation in *gstu38* plants may have a negative effect on PepMV infection.

PepMV induced deeper transcriptomic changes in WT plants as compared to *gstu38* plants (Table S7). This may occur because there is a higher accumulation of PepMV in WT plants and also because healthy WT and *gstu38* plants have different transcriptome profiles and different signaling pathways activated. The description of expression patterns of specific PepMV-DEGs allowed us to identify genes overexpressed in infected WT plants and downregulated in infected *gstu38* plants (cluster 4), and genes exclusively overexpressed in infected *gstu38* plants (cluster 6). We reasoned that clusters 4 and 6 could be enriched in genes with proviral or antiviral functions, respectively. In cluster 4, four out of 16 genes encoded proteins predicted to have immune response functions (Table 1, genes marked in orange). In cluster 6, out of 14 genes, three were predicted by homology to be positively regulated by the ABA signaling pathway, and two by SA

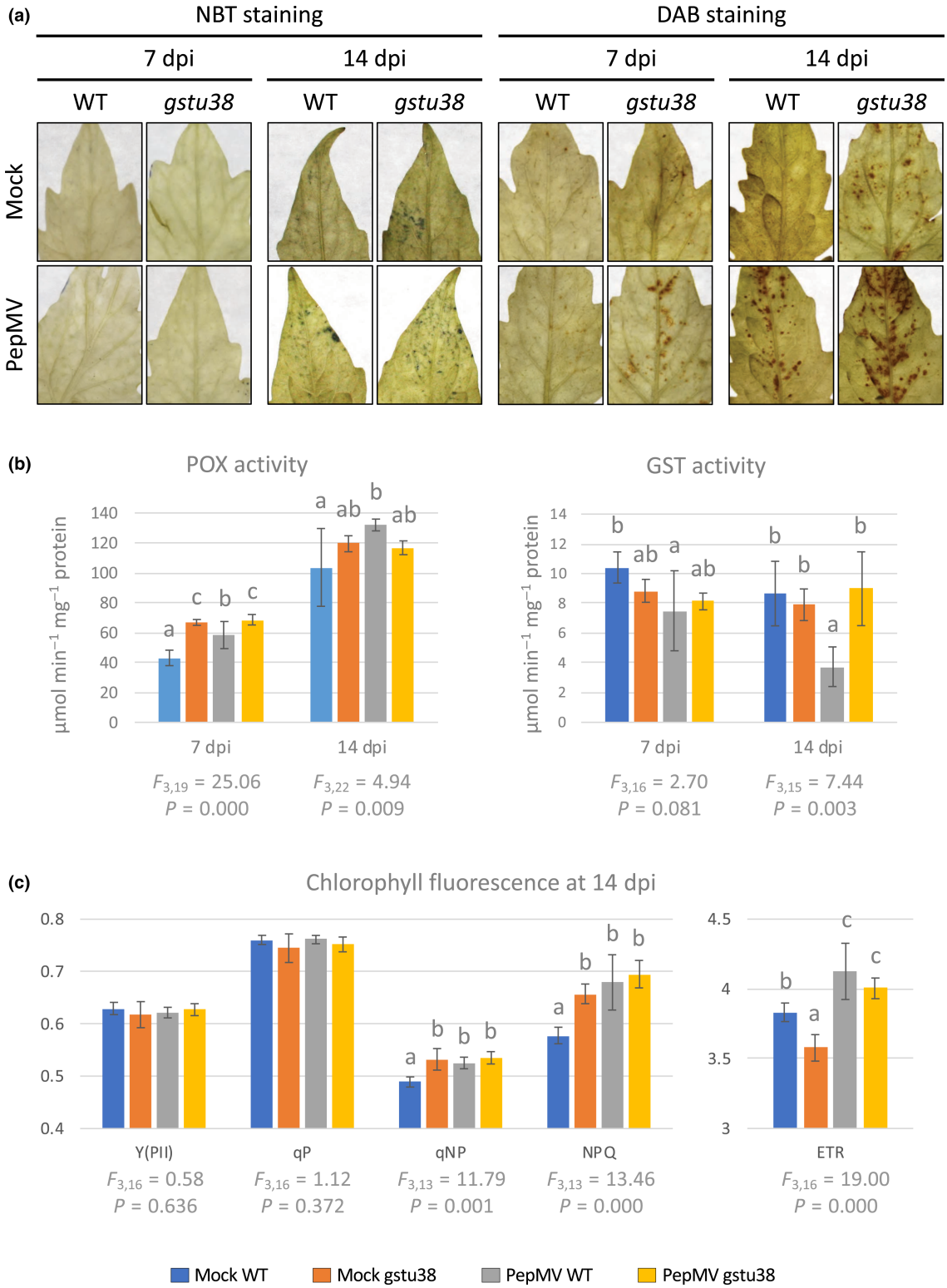

Fig. 8 Effect of Pepino mosaic virus (PepMV) infection and SlGSTU38 knockout on reactive oxygen species (ROS) accumulation, peroxidase and glutathione *S*-transferase activities, and chlorophyll fluorescence in Micro-Tom leaves. (a) Histochemical staining with nitro blue tetrazolium (NBT) and diaminobenzidine (DAB) of leaves from healthy (Mock) and PepMV-infected wild-type (WT) and *gstu38* plants at 7- and 14-d postinoculation (dpi). NBT and DAB staining show more superoxide or hydrogen peroxide accumulation, respectively, in healthy *gstu38* and PepMV-infected WT or *gstu38* leaves compared with healthy WT leaves. (b, c) Bar plots representing means of (b) peroxidase (POX) and glutathione *S*-transferase (GST) activity and (c) chlorophyll fluorescence parameters of each treatment. Error bars represent the SD. Letters indicate statistically significant differences between treatments computed by one-way ANOVA and Duncan's multiple range test. *F*-ratio ($F_{x,y}$) and *P*-value (*P*) of each analysis are indicated below bar plots. ETR, electron transport rate; NPQ and qNP, nonphotochemical quenching parameters; qP, photochemical quenching; Y(PSII), quantum yield of PSII.

(Table 1, genes marked in green or blue, respectively). The upregulation of ABA-induced genes in infected *gstu38* plants is consistent with the downregulation of negative regulators of the ABA response in healthy *gstu38* plants. In addition, a DNA REPAIR AND RECOMBINATION PROTEIN, and a gene encoding a co-chaperone DNAJ subtype DNAJC (Pulido & Leister, 2018) were included in cluster 6 (Table 1, genes marked in blue). Both protein families have been shown to be involved in responses to virus infection (Cho *et al.*, 2012; Kaliappan *et al.*, 2012; Liu *et al.*, 2022). Further analyses focusing on cluster 6 genes may contribute to a better understanding of why *gstu38* plants are less susceptible to PepMV.

Plants edited in *SlGSTU38* may be of potential interest for tomato breeding; while they are partially resistant to PepMV, they do not have any other obvious phenotypes associated with the mutation in spite of having upregulated SA-induced genes. However, some important questions remain: We do not know how the deregulation of stress-related genes could affect the *gstu38* plants' response against abiotic stresses or other pathogens or pests, and the partial resistance to PepMV may need to be pyramided to other PepMV resistance genes. Clearly, before their practical application, further research needs to be done with the *gstu38* plants.

Acknowledgements

We thank Mª Carmen Montesinos (CEBAS-CSIC, Spain) and Fátima Valle Barea (CEBAS-CSIC, Spain) for their help with growing plants; Luis Rodríguez-Moreno (Málaga University, Spain) for preparing the CP construct for the initial Y2H screening; and Mario Fon (*mariogfon@gmail.com*) for editing the manuscript. This work was supported by grants RTI2018-097099-B-I00 and PID2021-125010OB-I00 from Ministerio de Ciencia e Innovación (Spain). EM-L was supported by grant BES-2013-064540 (Ministerio de Ciencia e Innovación; Spain). Work in JT laboratory was supported by the Scottish Government's Rural and Environment Science and Analytical Services Division (RESAS).

Competing interests

None declared.

Author contributions

MAA, EM-L, and LD conceived the study. EM-L and LD generated the DNA constructs. EM-L and LD performed the directed Y2H assay. EM-L and JT performed the CoIP assay. BG transformed Micro-Tom plants. EM-L, LD, and BG performed the virus susceptibility analyses. EM-L, JT, and MAS-P contribute to the live-cell confocal imaging study. LD and EM-L performed the RNA-seq study. PD-V and EM-L performed enzymatic assays, lipid peroxidation determination, the histochemical staining and the chlorophyll fluorescence. EM-L and MAA wrote the paper with input from all co-authors.

ORCID

Miguel A. Aranda https://orcid.org/0000-0002-0828-973X
Pedro Díaz-Vivancos https://orcid.org/0000-0001-6041-2128
Livia Donaire https://orcid.org/0000-0002-5454-2994
Blanca Gosálvez https://orcid.org/0000-0001-5989-7148
Eduardo Méndez-López https://orcid.org/0000-0002-0797-7661
M. Amelia Sánchez-Pina https://orcid.org/0000-0002-3648-5666
Jens Tilsner https://orcid.org/0000-0003-3873-0650

Data availability

The data that support the findings of this study are available from the corresponding author upon reasonable request.

References

Agirrezabala X, Méndez-López E, Lasso G, Sánchez-Pina MA, Aranda M, Valle M. 2015. The near-atomic cryoEM structure of a flexible filamentous plant virus shows homology of its coat protein with nucleoproteins of animal viruses. *eLife* **4**: 1–11.

Agüero J, Gómez-Aix C, Sempere RN, García-Villalba J, García-Núñez J, Hernando Y, Aranda MA. 2018. Stable and broad spectrum cross-protection against Pepino mosaic virus attained by mixed infection. *Frontiers in Plant Science* **9**: 01810.

Aguilar JM, Hernández-Gallardo MD, Cenis JL, Lacasa A, Aranda MA. 2002. Complete sequence of the Pepino mosaic virus RNA genome. *Archives of Virology* **147**: 2009–2015.

Alcaide C, Donaire L, Aranda MA. 2022. Transcriptome analyses unveiled differential regulation of AGO and DCL genes by Pepino mosaic virus strains. *Molecular Plant Pathology* **23**: 1592–1607.

Anders S, Huber W. 2010. Differential expression analysis for sequence count data. *Genome Biology* **11**: R106.

Andrews S. 2010. *FASTQC: a quality control tool for high throughput sequence data.* [WWW document] URL http://www.bioinformatics.babraham.ac.uk/projects/fastqc/ [accessed 4 October 2021].

Bartling D, Radzio R, Steiner U, Weiler EW. 1993. A glutathione *S*-transferase with glutathione-peroxidase activity from *Arabidopsis thaliana. European Journal of Biochemistry* **216**: 579–586.

Bartoli CG, Casalongué CA, Simontacchi M, Marquez-Garcia B, Foyer CH. 2013. Interactions between hormone and redox signalling pathways in the control of growth and cross tolerance to stress. *Environmental and Experimental Botany* **94**: 73–88.

Bolger AM, Lohse M, Usadel B. 2014. TRIMMOMATIC: a flexible trimmer for Illumina sequence data. *Bioinformatics* **30**: 2114–2120.

Candresse T, Marais A, Faure C, Dubrana MP, Gombert J, Bendahmane A. 2010. Multiple coat protein mutations abolish recognition of *Pepino mosaic potexvirus* (PepMV) by the potato *Rx* resistance gene in transgenic tomatoes. *Molecular Plant–Microbe Interactions* **23**: 376–383.

Chen IH, Chiu MH, Cheng SF, Hsu YH, Tsai CH. 2013. The glutathione transferase of *Nicotiana benthamiana* NbGSTU4 plays a role in regulating the early replication of Bamboo mosaic virus. *New Phytologist* **199**: 749–757.

Cho SY, Cho WK, Sohn SH, Kim KH. 2012. Interaction of the host protein NbDnaJ with Potato virus X minus-strand stem-loop 1 RNA and capsid protein affects viral replication and movement. *Biochemical and Biophysical Research Communications* **417**: 451–456.

Choi H, Cho WK, Kim K. 2016. Two homologous host proteins interact with potato virus X RNAs and CPs and affect viral replication and movement. *Scientific Reports* **6**: 28743.

Díaz-Vivancos P, Clemente-Moreno MJ, Rubio M, Olmos E, García JA, Martínez-Gómez P, Hernández JA. 2008. Alteration in the chloroplastic metabolism leads to ROS accumulation in pea plants in response to plum pox virus. *Journal of Experimental Botany* **59**: 2147–2160.

Dixon DP, Hawkins T, Hussey PJ, Edwards R. 2009. Enzyme activities and subcellular localization of members of the Arabidopsis glutathione transferase superfamily. *Journal of Experimental Botany* **60**: 1207–1218.

Eck JV, Kirk DD, Walmsley AM. 2006. Tomato (*Lycopersicum esculentum*). In: Wang K, ed. *Agrobacterium protocols. Methods in molecular biology, vol. 343*. Clifton, NJ, USA: Humana Press, 459–473.

Feng N, Song G, Guan J, Chen K, Jia M, Huang D, Wu J, Zhang L, Kong X, Geng S *et al.* 2017. Transcriptome profiling of wheat inflorescence development from spikelet initiation to floral patterning identified stage-specific regulatory Genes. *Plant Physiology* **174**: 1779–1794.

Fernandez-Pozo N, Menda N, Edwards JD, Saha S, Tecle IY, Strickler SR, Bombarely A, Fisher-York T, Pujar A, Foerster H *et al.* 2015. The Sol Genomics Network (SGN)-from genotype to phenotype to breeding. *Nucleic Acids Research* **43**: D1036–D1041.

García-Alcalde F, Okonechnikov K, Carbonell J, Cruz LM, Götz S, Tarazona S, Dopazo J, Meyer TF, Conesa A. 2012. Qualimap: evaluating next-generation sequencing alignment data. *Bioinformatics* **28**: 2678–2679.

Gietz RD, Schiestl RH. 1994. Transforming yeast with DNA. *Methods in Molecular and Cellular Biology* **5**: 255–269.

Gómez P, Sempere RN, Aranda MA. 2012. Pepino mosaic virus and tomato torrado virus. Two emerging viruses affecting tomato crops in the mediterranean basin. *Advances in Virus Research* **84**: 505–532.

Grek CL, Zhang J, Manevich Y, Townsend DM, Tew KD. 2013. Causes and consequences of cysteine *s*-glutathionylation. *Journal of Biological Chemistry* **288**: 26497–26504.

Gullner G, Komives T, Király L, Schröder P. 2018. Glutathione *S*-transferase enzymes in plant–pathogen interactions. *Frontiers in Plant Science* **9**: 01836.

Hanssen IM, Guriérrez-Aguirre I, Paeleman A, Goen K, Wittemans L, Lievens B, Vanachter ACRC, Ravnikar M, Thomma BPHJ. 2010. Cross-protection or enhanced symptom display in greenhouse tomato co-infected with different Pepino mosaic virus isolates. *Plant Pathology* **59**: 13–21.

Hanssen IM, Thomma BPHJ. 2010. Pepino mosaic virus: a successful pathogen that rapidly evolved from emerging to endemic in tomato crops. *Molecular Plant Pathology* **11**: 179–189.

Huang YW, Hu CC, Lin NS, Hsu YH. 2012. Unusual roles of host metabolic enzymes and housekeeping proteins in plant virus replication. *Current Opinion in Virology* **2**: 676–682.

Husain T, Fatima A, Suhel M, Singh S, Sharma A, Prasad SM, Singh VP. 2020. A brief appraisal of ethylene signaling under abiotic stress in plants. *Plant Signaling and Behavior* **15**: e1782051.

Islam S, Rahman IA, Islam T, Ghosh A. 2017. Genome-wide identification and expression analysis of glutathione *S*-transferase gene family in tomato: gaining an insight to their physiological and stress-specific roles. *PLoS ONE* **12**: 0187504.

Kaliappan K, Choudhury NR, Suyal G, Mukherjee SK. 2012. A novel role for RAD54: this host protein modulates geminiviral DNA replication. *The FASEB Journal* **26**: 1142–1160.

Karpiński S, Szechyńska-Hebda M, Wituszyńska W, Burdiak P. 2013. Light acclimation, retrograde signalling, cell death and immune defences in plants. *Plant, Cell & Environment* **36**: 736–744.

Kocsy G, Tari I, Vanková R, Zechmann B, Gulyás Z, Poór P, Galiba G. 2013. Redox control of plant growth and development. *Plant Science* **211**: 77–91.

Li H, Durbin R. 2009. Fast and accurate short read alignment with Burrows-Wheeler transform. *Bioinformatics* **25**: 1754–1760.

Liang G, Zhang H, Lou D, Yu D. 2016. Selection of highly efficient sgRNAs for CRISPR/Cas9-based plant genome editing. *Scientific Reports* **6**: 21451.

Liao Y, Smyth GK, Shi W. 2019. The R package Rsubread is easier, faster, cheaper and better for alignment and quantification of RNA sequencing reads. *Nucleic Acids Research* **47**: e47.

Lim HS, Nam J, Seo EY, Nam M, Vaira AM, Bae H, Jang CY, Lee CH, Kim HG, Roh M *et al.* 2014. The coat protein of Alternanthera mosaic virus is the elicitor of a temperature-sensitive systemic necrosis in *Nicotiana benthamiana*, and interacts with a host boron transporter protein. *Virology* **452–453**: 264–278.

Liu T, Xu M, Gao S, Zhang Y, Hu Y, Jin P, Cai L, Cheng Y, Chen J, Yang J *et al.* 2022. Genome-wide identification and analysis of the regulation wheat DnaJ family genes following wheat yellow mosaic virus infection. *Journal of Integrative Agriculture* **21**: 153–169.

Love MI, Huber W, Anders S. 2014. Moderated estimation of fold change and dispersion for RNA-seq data with DESeq2. *Genome Biology* **15**: 550.

Lu Q, Tang X, Tian G, Wang F, Liu K, Nguyen V, Kohalmi SE, Keller WA, Tsang EWT, Harada JJ *et al.* 2010. Arabidopsis homolog of the yeast TREX-2 mRNA export complex: components and anchoring nucleoporin. *The Plant Journal* **61**: 259–270.

Martinoia E, Grill E, Tommasini R, Kreuz K, Amrhein N. 1993. ATP-dependent glutathione *S*-conjugate 'export' pump in the vacuolar membrane of plants. *Nature* **364**: 247–249.

Mathioudakis M, Khechmar S, Owen C, Medina V, Ben Mansour K, Tomaszewska W, Spanos T, Sarris P, Livieratos I. 2018. A thioredoxin domain-containing protein interacts with Pepino mosaic virus triple gene block protein 1. *International Journal of Molecular Sciences* **19**: 3747.

Mathioudakis MM, Rodríguez-Moreno L, Sempere RN, Aranda MA, Livieratos I. 2014. Multifaceted capsid proteins: multiple interactions suggest multiple roles for *Pepino mosaic virus* capsid protein. *Molecular Plant–Microbe Interactions* **27**: 1356–1369.

Mathioudakis MM, Veiga R, Ghita M, Tsikou D, Medina V, Canto T, Makris AM, Livieratos IC. 2012. Pepino mosaic virus capsid protein interacts with a tomato heat shock protein cognate 70. *Virus Research* **163**: 28–39.

Mathioudakis MM, Veiga RSL, Canto T, Medina V, Mossialos D, Makris AM, Livieratos I. 2013. Pepino mosaic virus triple gene block protein 1 (TGBp1) interacts with and increases tomato catalase 1 activity to enhance virus accumulation. *Molecular Plant Pathology* **14**: 589–601.

Minicka J, Otulak K, Garbaczewska G, Pospieszny H, Hasiów-Jaroszewska B. 2015. Ultrastructural insights into tomato infections caused by three different pathotypes of Pepino mosaic virus and immunolocalization of viral coat proteins. *Micron* **79**: 84–92.

Moreau S, Van Aubel G, Janky R, Van Cutsem P. 2020. Chloroplast electron chain, ROS production, and redox homeostasis are modulated by COS-OGA elicitation in tomato (*Solanum lycopersicum*) leaves. *Frontiers in Plant Science* **11**: 597589.

Nakagawa T, Kurose T, Hino T, Tanaka K, Kawamukai M, Niwa Y, Toyooka K, Matsuoka K, Jinbo T, Kimura T. 2007a. Development of series of gateway binary vectors, pGWBs, for realizing efficient construction of fusion genes for plant transformation. *Journal of Bioscience and Bioengineering* **104**: 34–41.

Nakagawa T, Suzuki T, Murata S, Nakamura S, Hino T, Maeo K, Tabata R, Kawai T, Tanaka K, Niwa Y *et al.* 2007b. Improved gateway binary vectors: high-performance vectors for creation of fusion constructs in transgenic analysis of plants. *Bioscience, Biotechnology and Biochemistry* **71**: 2095–2100.

Nguyen-Dinh V, Herker E. 2021. Ultrastructural features of membranous replication organelles induced by positive-stranded RNA viruses. *Cell* **10**: 2407.

Nieto C, Rodríguez-Moreno L, Rodríguez-Hernández AM, Aranda MA, Truniger V. 2011. Nicotiana benthamiana resistance to non-adapted Melon necrotic spot virus results from an incompatible interaction between virus RNA and translation initiation factor 4E. *The Plant Journal* **66**: 492–501.

Oliveros JC, Franch M, Tabas-Madrid D, San-León D, Montoliu L, Cubas P, Pazos F. 2016. Breaking-Cas-interactive design of guide RNAs for CRISPR-Cas experiments for ENSEMBL genomes. *Nucleic Acids Research* **44**: W267–W271.

Padmanabhan M, Cournoyer P, Dinesh-Kumar SP. 2009. The leucine-rich repeat domain in plant innate immunity: a wealth of possibilities. *Cellular Microbiology* **11**: 191–198.

Park M-R, Jeong R-D, Kim K-H. 2014. Understanding the intracellular trafficking and intercellular transport of potexviruses in their host plants. *Frontiers in Plant Science* **5**: 60.

Park M-R, Kim K-H. 2013. Molecular characterization of the interaction between the N-terminal region of Potato virus X (PVX) coat protein (CP) and *Nicotiana benthamiana* PVX CP-interacting protein, NbPCIP1. *Virus Genes* **46**: 517–523.

Pechar GS, Donaire L, Gosalvez B, Garc C, Amelia S, Aranda MA. 2022. Editing melon eIF4E associates with virus resistance and male sterility. *Plant Biotechnology Journal* **20**: 2006–2022.

Pulido P, Leister D. 2018. Novel DNAJ-related proteins in *Arabidopsis thaliana*. *New Phytologist* **217**: 480–490.

Riyazuddin R, Verma R, Singh K, Nisha N, Keisham M, Bhati KK, Kim ST, Gupta R. 2020. Ethylene: a master regulator of salinity stress tolerance in plants. *Biomolecules* **10**: 959.

Ruiz-Ramón F, Sempere RN, Méndez-López E, Sánchez-Pina MA, Aranda MA. 2019. Second generation of Pepino mosaic virus vectors: improved stability in tomato and a wide range of reporter genes. *Plant Methods* **15**: 58.

Sánchez-Pina MA, Gómez-Aix C, Méndez-López E, Gosalvez-Bernal B, Aranda MA. 2021. Imaging techniques to study plant virus replication and vertical transmission. *Viruses* **13**: 358.

Sempere RN, Gómez P, Truniger V, Aranda MA. 2011. Development of expression vectors based on Pepino mosaic virus. *Plant Methods* **7**: 6.

Sempere RN, Gómez-Aix C, Ruíz-Ramón F, Gómez P, Hasiów-Jaroszewska B, Sánchez-Pina MA, Aranda MA. 2016. Pepino mosaic virus RNA-dependent RNA polymerase POL domain is a hypersensitive response-like elicitor shared by necrotic and mild isolates. *Phytopathology* **106**: 395–406.

Soler-Aleixandre S, López C, Cebolla-Cornejo J, Nuez F. 2007. Sources of resistance to Pepino mosaic virus (PepMV) in tomato. *HortScience* **42**: 40–45.

Tilsner J, Linnik O, Louveaux M, Roberts IM, Chapman SN, Oparka KJ. 2013. Replication and trafficking of a plant virus are coupled at the entrances of plasmodesmata. *Journal of Cell Biology* **201**: 981–995.

Tilsner J, Linnik O, Wright KM, Bell K, Roberts AG, Lacomme C, Santa Cruz S, Oparka KJ. 2012. The TGB1 movement protein of potato virus X reorganizes actin and endomembranes into the X-body, a viral replication factory. *Plant Physiology* **158**: 1359–1370.

Vaish S, Gupta D, Mehrotra R, Mehrotra S, Basantani MK. 2020. Glutathione *S*-transferase: a versatile protein family. *3 Biotech* **10**: 321.

Vishwakarma K, Upadhyay N, Kumar N, Yadav G, Singh J, Mishra RK, Kumar V, Verma R, Upadhyay RG, Pandey M *et al.* 2017. Abscisic acid signaling and abiotic stress tolerance in plants: a review on current knowledge and future prospects. *Frontiers in Plant Science* **8**: 00161.

van der Vlugt RAA, Cuperus C, Vink J, Stijger ICMM, Lesemann DE, Verhoeven JTJ, Roenhorst JW. 2002. Identification and characterization of Pepino mosaic potexvirus in tomato. *EPPO Bulletin* **32**: 503–508.

van der Vlugt RAA, Stijger CCMM, Verhoeven JTJ, Lesemann D-E. 2000. First report of Pepino mosaic virus on tomato. *Plant Disease* **84**: 103.

Wagner U, Edwards R, Dixon DP, Mauch F. 2002. Probing the diversity of the *Arabidopsis glutathione S*-transferase gene family. *Plant Molecular Biology* **49**: 515–532.

Zamora M, Méndez-López E, Agirrezabala X, Cuesta R, Lavín JL, Amelia Sánchez-Pina M, Aranda MA, Valle M. 2017. Potyvirus virion structure shows conserved protein fold and RNA binding site in ssRNA viruses. *Science Advances* **3**: 1–8.

Zuker M. 2003. Mfold web server for nucleic acid folding and hybridization prediction. *Nucleic Acids Research* **31**: 3406–3415.

Supporting Information

Additional Supporting Information may be found online in the Supporting Information section at the end of the article.

Fig. S1 Yeast two-hybrid screening of a cDNA normalized tomato library against the CP of PepMV and identification of SlGSTU38 as a possible CP-interacting protein.

Fig. S2 Phylogenetic relationship of SlGSTU38 and its homologs.

Fig. S3 Mock-inoculated and PepMV-infected WT and gstu38 Micro-Tom plants at 14-d postinoculation.

Fig. S4 Subcellular localization and colocalization of CP and SlGSTU38.

Fig. S5 RNA-seq data validation.

Fig. S6 PepMV or SlGSTU38 knockout do not induce lipid peroxidation in Micro-Tom plants.

Methods S1 Tomato cDNA library and yeast two-hybrid screening.

Table S1 Primer sequences.

Table S2 Construct summary.

Table S3 BLASTp output using the SlGSTU38 protein sequence as query in the Sol Genomics Network database.

Table S4 RNA-seq results: number of expressed genes per treatment and in all treatments together.

Table S5 RNA-seq results: genes exclusively expressed in mock-inoculated gstu38 (gstu38_M), mock-inoculated wild-type (WT_M), and PepMV-inoculated wild-type plants (WT_PepMV).

Table S6 RNA-seq results: number of differentially expressed genes (DEGs) for all the possible pairwise comparisons between treatments.

Table S7 Differentially expressed genes (DEGs) comparing mock-inoculated gstu38 with mock-inoculated wild-type (WT) plants.

Please note: Wiley is not responsible for the content or functionality of any Supporting Information supplied by the authors. Any queries (other than missing material) should be directed to the *New Phytologist* Central Office.